Multistage Strategies to Incorporate Phasor Measurements into Power System State Estimation

André Albuquerque, Daniel Bez, Antonio Simões Costa
Power Systems Group, Federal University of Santa Catarina, Brazil

Abstract

This paper presents two novel estimation architectures to combine SCADA and PMU measurements into multistage strategies for Power System State Estimation. The first architecture makes use of *a priori* state information concepts and a blocked version of orthogonal Givens rotations with the objective of enhancing SCADA based estimates through PMU data processing. The second strategy is a three-stage scheme that relies on estimation fusion principles to optimally combine previously determined SCADA- and PMU-based estimates. In either case, observability with respect to PMU measurements is not assumed. multistage methods are described in detail and their computational requirements and properties are discussed. Results obtained for two IEEE test systems are used to illustrate the application of the estimation strategies.

I. Introduction

DURING the last several decades, Power System State Estimation (PSSE) has established itself as the basic tool for real-time modeling of large electric power networks. As the emerging Smart Grid concepts expand previous paradigms for power system operation and control, PSSE must evolve to keep pace with the current trends [1]. This requires the incorporation of new technologies to fulfill more stringent accuracy and observability requirements posed to state estimators. Conventional state estimators process data gathered by SCADA systems by scanning remote terminal units (RTUs) located at the power system substations. The advent of the phasor measurement technology has made it possible to accurately measure bus voltage and branch current phasors, something previously infeasible with SCADA. As a consequence, the use of Phasor Measurement Units (PMUs) in power system state estimation has deserved much attention in recent years.

The question then arises as whether SCADA technology should be simply replaced by PMU systems. Several arguments can be raised to argue otherwise, such as the insufficient number of PMU measurements usually available to provide full system observability, and the existence of complex SCADA infrastructures deployed along many years that should not be simply discarded. Hence, it does not seem feasible to consider the full replacement of the SCADA infrastructure by PMUs, at least in the near future. A more sensible solution is to combine the widespread availability of conventional measurements with the enhanced quality of observations provided by the PMU technology. For that purpose, however, one faces the problem of how to conceive state estimation strategies able to benefit from both technologies.

A possible solution for this problem is to consider state estimators able to simultaneously process both SCADA and PMU measurements. This is a centralized strategy, since all gathered data, regardless of the underlying technology, are processed by the same estimation module. Although that can be seen as an extension of conventional estimation algorithms in order to enable phasor measurement processing, significant changes in the software are required. The resulting estimator, often referred to as Hybrid Simultaneous State Estimator, has produced successful results, as shown in the literature [2], [3], [4], [5], [6]. In spite of that, it is unlikely that utilities and system operators that currently run SCADA-based estimators will be willing to replace their EMS software in order accommodate the necessary structural changes. Furthermore, some existing estimators are based on decoupled algorithms which are not readily able to process electric current phasor measurements.

To address that issue, novel state estimation structures in which phasor measurements are processed in a second estimation stage have been recently proposed in the literature [7], [8], [9]. Those *multistage state estimators* allow that conventional SCADA-based estimators be kept unchanged while preserving the benefits of PMU measurements to the overall state estimation process.

Two distinct and recently proposed multistage estimation approaches to combine SCADA and PMU-based data are addressed in this paper. The first estimation architecture relies on the *a priori* state information (APSI) concept and takes advantage of the three-multiplier Givens rotations ability to accommodate that kind of information at virtually no extra computational cost [10]. Accordingly, SCADA-based state estimates obtained from the first estimation stage are treated by the second, PMU-based estimation module, as *a priori* state information. It is thereby expected that the APSI hybrid estimator will enhance the quality of the conventional estimates through the processing of the available phasor measurements [8],[6].

The second multistage estimation method is based on Multisensor Data Fusion Theory, a relatively recent research field

978-1-4799-0199-9/13/ $31.00 ©2013 IEEE

pertaining to the Data and Signal Processing area [11]. According to this approach, distinct state estimates are obtained by separate SCADA- and PMU-based estimation modules. Those estimates are then combined in a fusion center, thus producing a final vector of optimal estimates [9].

Both multistage architectures will be described in detail, along with their distinguished properties and implementation issues. The contribution of phasor measurements to enhance bad data processing capability will be also investigated. Case studies performed on distinct IEEE benchmark systems will be used to evaluate and compare the proposed strategies.

This paper is organized as follows. The basic PSSE principles and concepts needed to describe the novel estimation strategies are reviewed in Section II. The APSI approach based on Blocked Givens rotations is presented in Section III, while Section IV describes the Estimation Fusion estrategy. Results of case studies conducted on the IEEE 30-bus and 57-bus test systems are presented and discussed in Section VI. Finally, Section VII summarizes the paper contents and lists some the concluding remarks.

II. State Estimation Background

A.Weighted Least Squares Estimator

State estimation performs power system real-time modeling by processing real-time data gathered from remote meters. Assuming that a set of m measurements are gathered from an N bus power network, the relationship between measured quantities and the $n = 2N - 1$ state variables can be described by the following nonlinear measurement model:

$$\mathbf{z} = \mathbf{h}(\mathbf{x}) + \boldsymbol{\varepsilon} \tag{1}$$

where $\mathbf{z}$ is the $m \times 1$ measurement vector, $\mathbf{x}$ is the $n \times 1$ vector of state variables to be estimated, $\mathbf{h}(\mathbf{x})$ is the $m \times 1$ vector of nonlinear functions relating measured quantities and state variables, and $\boldsymbol{\varepsilon}$ is the $m \times 1$ measurement error vector, whose $m \times m$ covariance matrix is denoted by $\mathbf{R}$. Under the usual assumption that measurements are uncorrelated, matrix $\mathbf{R}$ is diagonal and its *i-th* diagonal entry is the variance of the error of measurement i, denoted by σ_i^2.

The Weighted Least-Squares (WLS) approach to the PSSE problem is based on the minimization of the weighted sum of the squared residuals:

$$\min_{\hat{\mathbf{x}}} \; J(\hat{\mathbf{x}}) = \frac{1}{2} \left[\mathbf{z} - \mathbf{h}(\hat{\mathbf{x}})\right]^t \mathbf{R}^{-1} \left[\mathbf{z} - \mathbf{h}(\hat{\mathbf{x}})\right]. \tag{2}$$

The above problem can be solved through the Gauss-Newton method, leading to an iterative process in which the so-called *normal equation* is solved in each iteration [12], [13], [14]:

$$\mathbf{G} \; \boldsymbol{\Delta}\mathbf{x} = \mathbf{H}^t \; \mathbf{R}^{-1} \boldsymbol{\Delta}\mathbf{z} \tag{3}$$

where $\mathbf{G} = \left(\mathbf{H}^t \, \mathbf{R}^{-1} \, \mathbf{H}\right)$ is often referred to as the gain matrix; $\mathbf{H}$ is the $m \times n$ Jacobian matrix of $\mathbf{h}(\mathbf{x})$ computed at a given point $\mathbf{x}^k$, and $\boldsymbol{\Delta}\mathbf{z} = \mathbf{z} - \mathbf{h}(\mathbf{x}^k)$.

The solution of Eq. (3) yields vector $\boldsymbol{\Delta}\mathbf{x}$ of increments to the current vector of state estimates, so that the updated state vector is obtained as

$$\mathbf{x}^{k+1} = \mathbf{x}^k + \boldsymbol{\Delta}\mathbf{x} \tag{4}$$

The convergence of the iterative procedure is attained when $\boldsymbol{\Delta}\mathbf{x}$ becomes smaller than a pre-specified tolerance.

Upon convergence of the state estimator, the estimation error covariance matrix can be computed as

$$\mathbf{C}_x = \mathbf{G}^{-1} = \left(\mathbf{H}^t \, \mathbf{R}^{-1} \, \mathbf{H}\right)^{-1} \tag{5}$$

Matrix $\mathbf{C}_x$ provides a means for evaluating the degree of confidence on the accuracy of the state estimates [12].

B.A Priori State Information

Prior knowledge about the state variables is often available, and can be taken into account in the estimation process as *a priori* state information. For that purpose, a degree of confidence should be assigned to such data, under the form of a covariance matrix. *A priori* state information contributes to state estimation in a similar fashion as measured data, although in the proportion of the respective accuracies, as given by the corresponding variances.

If $\bar{\mathbf{x}}$ denotes the $n \times 1$ vector of *a priori* state values and $\mathbf{P}_0$ is the $n \times n$ corresponding covariance matrix, *a priori* information can be embedded into the WLS problem by augmenting the objective function (2) as [15]:

$$\begin{aligned} \min_{\hat{\mathbf{x}}} \; J(\hat{\mathbf{x}}) \;\; = \;\; & \tfrac{1}{2} \left[\mathbf{z} - \mathbf{h}(\hat{\mathbf{x}})\right]^t \mathbf{R}^{-1} \left[\mathbf{z} - \mathbf{h}(\hat{\mathbf{x}})\right] + \\ & \tfrac{1}{2} (\hat{\mathbf{x}} - \bar{\mathbf{x}})^t \mathbf{P}_0^{-1} (\hat{\mathbf{x}} - \bar{\mathbf{x}}). \end{aligned} \tag{6}$$

It is often assumed that $\mathbf{P}_0 = \text{diag}\ \{\bar{\sigma}_1^2, \bar{\sigma}_2^2, \ldots, \bar{\sigma}_n^2\}$, and $\bar{\sigma}_i^2$ is the variance assigned to $\bar{x}_i$. The optimality conditions for Problem (6) lead to the following extended version of the normal equation [15]:

$$\left[\mathbf{H}^t \, \mathbf{R}^{-1} \, \mathbf{H} + \mathbf{P}_0^{-1}\right] \boldsymbol{\Delta}\mathbf{x} = \mathbf{H}^t \, \mathbf{R}^{-1} \boldsymbol{\Delta}\mathbf{z} + \mathbf{P}_0^{-1} \boldsymbol{\Delta}\bar{\mathbf{x}} \tag{7}$$

where $\boldsymbol{\Delta}\bar{\mathbf{x}} \triangleq \left(\bar{\mathbf{x}} - \mathbf{x}^k\right)$.

III. Two-Stage APSI State Estimation

The structure of the hybrid APSI state estimator is shown in Fig. 1. Its first estimation stage is simply a conventional state estimator based on SCADA measurements, with no extra restrictions imposed. The output of this module comprises the SCADA-based estimated state vector, $\hat{\mathbf{x}}_S$ and the corresponding estimation error covariance matrix, $\mathbf{C}_{x_S}$, computed as given by Eq. (5). Those are treated as *a priori* information by the second estimation stage, which processes phasor measurements only. A particular attractive feature of such strategy

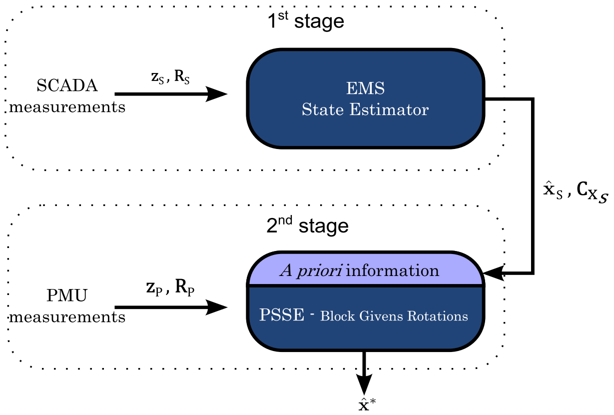

Fig. 1. Architecture of the APSI estimator.

is that it maintains intact the structure already in place with existing SCADA-based state estimators [8],[6].

In the heart of this scheme is the orthogonal estimator based on the three-multiplier version of Givens rotations (G3M) that constitutes the second stage. As shown in the sequel, the G3M estimator is able to process *a priori* information without any extra computational cost. Nevertheless, additional issues arise when one wishes to take full advantage of phasor data without significantly compromising the theoretical properties of the solution. Specifically, those issues are related to the steps required for: *a)* exploiting the possibility of employing a *linear* state estimator in the second stage, and *b)* avoiding approximations that may put at risk the desired statistical characteristics of the final estimates. Those topics are dealt with in the following subsections.

A.Three Multiplier scalar Givens rotations (G3M)

Consider the linearized version of the least-squares problem (2) with measurement model $\mathbf{z} = \mathbf{Hx} + \varepsilon$. Assume that an initial measurement vector $\mathbf{z}_0$ is selected which has the same size of the state vector, so that the corresponding observation matrix $\mathbf{H_0}$ is square. In addition, assume also that a new measurement z_1, related to the state variables as $z_1 = \mathbf{h}_1^t\mathbf{x}+\eta_1$, is to be processed. The rows of $\mathbf{H}_0$ and $\mathbf{h}_1^t$ are scaled by factors $\mathbf{R}_0^{-1/2}$ and $w^{1/2}$, respectively. Then a sequence of plane (Givens) rotations $\mathbf{Q}$ can be applied to the scaled rows of the new observation matrix (augmented with the corresponding measurements) so that [16]:

$$\mathbf{Q}\left(\begin{bmatrix}\mathbf{R}_0^{-\frac{1}{2}} & \\ & w^{\frac{1}{2}}\end{bmatrix}\left[\begin{array}{c|c}\mathbf{H}_0 & \mathbf{z}_0\\ \mathbf{h}_1^t & z_1\end{array}\right]\right) = \left[\begin{array}{c|c}\mathbf{U} & \mathbf{c}\\ \mathbf{0} & e\end{array}\right] \quad (8)$$

where $\mathbf{U}$ is a $n \times n$ upper triangular matrix, $\mathbf{c}$ is a $n \times 1$ vector, $\mathbf{0}$ is a $1 \times n$ null vector and e is an scalar. The estimated state vector $\hat{\mathbf{x}}$ based on the processed measurements can be obtained by simply solving the following triangular system of equations:

$$\mathbf{U}\ \hat{\mathbf{x}} = \mathbf{c} \quad (9)$$

The three-multiplier version of Givens rotations is based on the factorization of matrix $\mathbf{U}$ as [17]

$$\mathbf{U} = \mathbf{D}^{\frac{1}{2}}\bar{\mathbf{U}}, \quad (10)$$

where $\mathbf{D}$ is diagonal and $\bar{\mathbf{U}}$ is a *unit* upper triangular matrix. In this method, each row of the Jacobian matrix (augmented by the corresponding entry of $\boldsymbol{\Delta}\mathbf{z}$) is processed at a time. To illustrate the *G3M* rotations, consider that a new row vector $\mathbf{v}$, which corresponds to a row of $[\mathbf{H} \mid \boldsymbol{\Delta}\mathbf{z}]$, undergoes rotations with a row vector $\mathbf{u}$ from the matrix $\mathbf{U}$:

$$\begin{array}{l}\mathbf{u} = [\ 0 \ \cdots \ 0 \ \ \sqrt{d} \ \ \cdots \ \ \sqrt{d}\bar{u}_k \ \ \cdots \ \ \sqrt{d}\bar{u}_{n+1}\ ]\\ \mathbf{v} = [\ 0 \ \cdots \ 0 \ \ \sqrt{w}v_i \ \ \cdots \ \ \sqrt{w}v_k \ \ \cdots \ \ \sqrt{w}v_{n+1}\ ]\end{array} \quad (11)$$

Both vectors have already been scaled according to (10), by scaling factors $\sqrt{d}$ and $\sqrt{w}$, respectively. After a single rotation, the $i-th$ entry of $\mathbf{v}$ is zeroed out and the row vectors take the form

$$\begin{array}{l}\mathbf{u}' = [\ 0 \ \cdots \ 0 \ \ \sqrt{d'} \ \ \cdots \ \ \sqrt{d'}\bar{u}'_k \ \ \cdots \ \ \sqrt{d'}\bar{u}'_{n+1}\ ]\\ \mathbf{v}' = [\ 0 \ \cdots \ 0 \ \ 0 \ \ \cdots \ \ \sqrt{w'}v'_k \ \ \cdots \ \ \sqrt{w'}v_{n+1}\ ]\end{array} \quad (12)$$

Next, elementary rotations are sequentially performed in order to zero out all non-zero entries of $\mathbf{v}$. This process introduces changes in $\mathbf{U}$, $\mathbf{c}$ and e after each rotation.

A relevant consequence of the scaling mechanism is that it allows the weighting of each new measurement without increasing the computational burden. In the PSSE application, proper weighting of measurement z_i is achieved when $w_i = \sigma_i^{-2}$.

In regard to factor d_i, its value at the initialization of the rotation process can be seen as the weight for the initial value of state variable *i* before any measurement is processed. In other words, $d_i^{(0)}$ corresponds to the weighting factor of the *a priori* information available about the states. From Subsection II-B, we then conclude that

$$d_i^{(0)} = \frac{1}{\bar{\sigma}_i^2} \quad (13)$$

where $\bar{\sigma}_i^2$ is the variance of the *a priori* information on the state variable i. If no *a priori* information is available about the states, then $d_i^{(0)} = 0$. From (10), this implies that $\mathbf{U}$ is initially a null triangular matrix. If, on the contrary, there is prior information on the states, d_i should be initialized as in equation (13), and vector $\mathbf{c}$ as the available *a priori* information, that is, $\mathbf{c} = \bar{\mathbf{x}}$.

In conclusion, the 3M Givens rotations can easily consider *a priori* information at the very initialization stage of the estimation process, with no extra computational cost. This method to solve WLS problems is superior to the normal equation approach in terms of numerical robustness [16].

APSI estimator using phasor data in polar coordinates

A possible form to implement the second state estimation stage depicted in Fig. 1 is to process phasor data in their original polar form representation [8]. In that case, magnitude and phase angle measurement errors for both bus voltage and branch current phasors may be assumed uncorrelated. As a consequence, the covariance matrix $\mathbf{R}$ of Section II-A, when restricted to the phasor measurements, remains diagonal. This enables the use of state estimators that operate on an scalar, individual basis, to process phasor measurements at the second stage.

On the other hand, approximations are required to deal with the SCADA-based estimate $\hat{\mathbf{x}}_S$ and its covariance matrix, $\mathbf{C}_{x_S}$, which are also inputs for the second stage estimator in Fig. 1. Since the G3M estimator weighting mechanism can only handle uncorrelated *a priori* information, the off-diagonal terms of $\mathbf{C}_{x_S}$ must be neglected. However, the effect of *a priori* state correlations is only marginal and the approximation is considered a mild one. It has been also adopted in [7] and [8].

The downside of representing phasor measurements in polar coordinates is mainly computational. Such a representation leads to a nonlinear measurement model such as the one given by Eq. (1), so that an iterative scheme is required to determine the final estimates. In contrast to that, it has been previously shown that a change to rectangular coordinates leads to a *linear* modified measurement model, from which state estimates can be directly computed without the need of iterations [18],[7].

APSI estimator using phasor data in rectangular coordinates

The above observation naturally raises the question as why not simply applying the G3M algorithm to the linear model that results from changing the coordinates to the rectangular framework. This is possible, but at the price of additional approximations that have an impact on the statistical properties of the solution. Since The G3M rotations consider a *scalar* weighting scheme in which the weight assigned to each measurement depends solely on its variance, possible cross-correlations between measurement errors must be neglected. Although acceptable in certain applications, such as conventional SCADA-based state estimation, such assumption implies a strong statistical simplification for others. This is the case when voltage and current phasor measurements converted to rectangular form are to be processed by the state estimator, since the real and imaginary parts of such phasors tend to be strongly correlated.

To circumvent that limitation, an extended *blocked form* of the 3M Givens rotations has been developed in connection with this research work in order to consider the covariance between two distinct measurement errors. The proposed extension enables the joint processing of two measurements at a time, which can thus be seen as statistically coupled together, since their weighting factor becomes the inverse of the 2×2 covariance matrix of the paired observations.

B.Blocked form of G3M rotations

Consider that phasor measurements are now organized in pairs, and that the errors for each pair are assumed *correlated*. This implies that the covariance matrix $\mathbf{R}$ is *block diagonal*, that is,

$$E(\eta\eta^t) = \mathbf{R} = \begin{bmatrix} \sigma_1^2 & c_{12} & & & & \\ c_{21} & \sigma_2^2 & & & & \\ & & \sigma_3^2 & c_{34} & & \\ & & c_{43} & \sigma_4^2 & & \\ & & & & \ddots & \ddots \\ & & & & \ddots & \ddots \end{bmatrix} \tag{14}$$

where σ_i^2 is the variance of measurement i of the pair and $c_{ij} = c_{ji}$ stands for the covariance between the pair components.

Equation (8), which prescribes how new measurements are processed by the G3M rotations, can now be generalized. Accordingly, vector $\mathbf{z}_1$ is now composed by a 2×1 pair of new measurements, which are related to the states by the $2 \times n$ matrix $\mathbf{H}_1$. The proposed blocked form of the rotations is then applied to matrix $[\mathbf{H_0}^t \mid \mathbf{H}_1^t]^t$ augmented by vector $[\mathbf{z_0}^t \mid \mathbf{z}_1^t]^t$ (both previously scaled by $\mathbf{R}_0^{-\frac{1}{2}}$ and $\mathbf{W}^{\frac{1}{2}}$) in order to obtain an upper triangular linear system of equations. If $\tilde{\mathbf{Q}}$ represents the matrix that stores the rotations in the new blocked form, we have:

$$\tilde{\mathbf{Q}} \left(\begin{bmatrix} \mathbf{R}_0^{-\frac{1}{2}} & \\ & \mathbf{W}^{\frac{1}{2}} \end{bmatrix} \left[\begin{array}{c|c} \mathbf{H}_0 & \mathbf{z}_0 \\ \mathbf{H}_1 & \mathbf{z}_1 \end{array} \right] \right) = \left[\begin{array}{c|c} \tilde{\mathbf{U}} & \tilde{\mathbf{c}} \\ \mathbf{0} & \tilde{\mathbf{e}} \end{array} \right] \tag{15}$$

where $\tilde{\mathbf{c}}$ is a $n \times 2$ vector, $\mathbf{0}$ is a $2 \times n$ null matrix, $\tilde{e}$ is a 2×2 matrix and $\tilde{\mathbf{U}}$ is a $n \times n$ upper triangular matrix with 2×2 block identities on its main diagonal.

The estimated state vector $\hat{\mathbf{x}}$ is obtain by solving the triangular system of equations by back substitution.

$$\tilde{\mathbf{U}}\ \hat{\mathbf{x}} = \tilde{\mathbf{c}}_1 \tag{16}$$

where $\tilde{\mathbf{c}}_1$ is the first column of $\tilde{\mathbf{c}}$.

The block form of the G3M rotations is based on the same factorization as in (10), but now $\mathbf{D}$ is block diagonal, that is,

$$\mathbf{U} = \begin{bmatrix} \mathbf{D}_1^{\frac{1}{2}} & & & \\ & \mathbf{D}_2^{\frac{1}{2}} & & \\ & & \ddots & \\ & & & \mathbf{D}_n^{\frac{1}{2}} \end{bmatrix} \times \begin{bmatrix} \mathbf{I}_{2\times2} & \tilde{\mathbf{u}}_{12} & \tilde{\mathbf{u}}_{13} & \cdots & \tilde{\mathbf{u}}_{1n} \\ & \mathbf{I}_{2\times2} & \tilde{\mathbf{u}}_{23} & \cdots & \tilde{\mathbf{u}}_{2n} \\ & & \mathbf{I}_{2\times2} & \cdots & \tilde{\mathbf{u}}_{3n} \\ & & & \ddots & \vdots \\ & & & & \mathbf{I}_{2\times2} \end{bmatrix} \tag{17}$$

where $\mathbf{D}_i^{\frac{1}{2}}$ and $\tilde{\mathbf{u}}_{jk}$ are 2×2 matrices and $\mathbf{I}_{2\times2}$ is a 2×2 identity matrix.

Suppose that a $2 \times n$ matrix $\tilde{\mathbf{v}}$, which correspond to a pair of statistically coupled measurements in $[\mathbf{H} \mid \mathbf{z}]$, should undergo rotations with a $2 \times n$ submatrix $\tilde{\mathbf{u}}$ of $\tilde{\mathbf{U}}$ in order to zero out block $\tilde{\mathbf{v}}_i$.

$$\begin{array}{l} \tilde{\mathbf{u}} = [\ \mathbf{0} \ \cdots \ \mathbf{0} \ \ \mathbf{D}^{\frac{1}{2}} \ \cdots \ \mathbf{D}^{\frac{1}{2}}\tilde{\mathbf{u}}_k \ \cdots \ \mathbf{D}^{\frac{1}{2}}\tilde{\mathbf{u}}_{n+1}\ ] \\ \tilde{\mathbf{v}} = [\ \mathbf{0} \ \cdots \ \mathbf{0} \ \ \mathbf{W}^{\frac{1}{2}}\tilde{\mathbf{v}}_i \ \cdots \ \mathbf{W}^{\frac{1}{2}}\tilde{\mathbf{v}}_k \ \cdots \ \mathbf{W}^{\frac{1}{2}}\tilde{\mathbf{v}}_{n+1}\ ] \end{array} \tag{18}$$

After a single block rotation, the row vectors take the form

$$\begin{array}{l}\tilde{\mathbf{u}}' = [\ \mathbf{0}\ \cdots\ \mathbf{0}\ \ \mathbf{D}'^{\frac{1}{2}}\ \cdots\ \mathbf{D}'^{\frac{1}{2}}\tilde{\mathbf{u}}'_k\ \cdots\ \mathbf{D}'^{\frac{1}{2}}\tilde{\mathbf{u}}'_{n+1}\ ] \\ \tilde{\mathbf{v}}' = [\ \mathbf{0}\ \cdots\ \mathbf{0}\ \ \mathbf{0}\ \cdots\ \mathbf{W}'^{\frac{1}{2}}\tilde{\mathbf{v}}'_k\ \cdots\ \mathbf{W}'^{\frac{1}{2}}\tilde{\mathbf{v}}'_{n+1}\ ]\end{array} \tag{19}$$

In analogy with the scalar form, the sequence of block rotations successively annihilates all nonzero blocks of $\tilde{\mathbf{v}}$. In this process, matrices $\tilde{\mathbf{U}}$, $\tilde{\mathbf{c}}$ and $\tilde{\mathbf{e}}$ are also updated.

The weighting mechanism employed in the blocked version of Givens rotations is analogous to its scalar form, but it exhibits the distinctive advantage of enabling the consideration of the statistical correlation between the two measurements being processed. This is accomplished by defining the 2×2 measurement weighting factor as:

$$\mathbf{W} = \begin{bmatrix} \sigma^2_{\mathcal{R}e} & c_{Re,Im} \\ c_{Im,Re} & \sigma^2_{Im} \end{bmatrix}^{-1} \tag{20}$$

where $\sigma^2_{\mathcal{R}e}$ and $\sigma^2_{\mathcal{I}m}$ are the variances of the real and imaginary parts of the phasor measurement being processed and $c_{Re,Im} = c_{Im,Re}$ are the corresponding covariance.

Similarly, the correlation between pairs of voltage components in the *a priori* state information vector can also be easily taken into account. To achieve this, the generalized weighting factor $\mathbf{D}$ of the block triangular matrix in (17) should be initialized as:

$$\mathbf{D}^{(0)} = \begin{bmatrix} \bar{\sigma}^2_{\mathcal{R}e} & \bar{c}_{\mathcal{R}e,\mathcal{I}m} \\ \bar{c}_{\mathcal{I}m,\mathcal{R}e} & \bar{\sigma}^2_{\mathcal{I}m} \end{bmatrix}^{-1} \tag{21}$$

where entries of matrix $\mathbf{D}^{(0)}$ are similar to those in (20) but refer to *a priori* state information. According to the architecture of Fig. 1, it is easy to conclude that the 2×2 blocks inverted in Eq. (21) are obtained from matrix $\mathbf{C}_{x_S}$ in rectangular form. In addition, vector $\tilde{\mathbf{c}}$ of (15) should contain the a priori state information values ordered as a sequence of bus voltage real and imaginary parts, that is:

$$\tilde{\mathbf{c}}_1 = \bar{\mathbf{x}} = \hat{\mathbf{x}}_S \tag{22}$$

IV. Estimation Fusion Methods

A.Background and Estimation Architecture

The second multistage estimation approach is inspired in Multisensor Data Fusion (MDF) theory, which aims at combining the data generated by distinct classes of sensors in an optimal manner, so that the quality of the resulting information on the monitored process is enhanced with respect to that obtained from any single type sensors. A branch of MDF of particular interest from the PSSE point of view is *decentralized estimation fusion*, which combines estimates based on data generated by distinct sets of sensors [11], [19], [20]. Figure 2 illustrates that particular fusion architecture.

To introduce the mathematical formulation of decentralized estimation fusion, consider that a particular process is monitored by N_s distinct sets of sensors. Based on the data available from each set, we assume that a $n \times 1$ vector of estimates

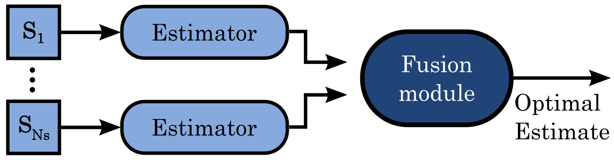

Fig. 2. Decentralized fusion estimator

$\hat{\mathbf{x}}_i$, $i = 1, \ldots, N_s$, is obtained for the state variables of the process. In addition, the resulting estimation errors can be correlated, so that the corresponding $n.N_s \times n.N_s$ covariance matrix is given by:

$$\mathbf{P} = \begin{bmatrix} P_{11} & \cdots & P_{1N_s} \\ \vdots & \ddots & \vdots \\ P_{N_s1} & \cdots & P_{N_sN_s} \end{bmatrix} \tag{23}$$

The optimal estimation fusion problem is obtained as a particular linear combination of the individual estimates $\hat{\mathbf{x}}_i$, that is

$$\hat{\mathbf{x}}^* = \mathbf{W}_1^t\ \hat{\mathbf{x}}_1 + \ldots + \mathbf{W}_{N_s}^t\ \hat{\mathbf{x}}_{N_s} \triangleq \mathbf{W}^t\ \hat{\mathbf{x}}_a \tag{24}$$

where $\mathbf{W}_1, \ldots, \mathbf{W}_{N_s}$ are $n \times n$ weighting matrices, $\mathbf{W} \triangleq \left[\mathbf{W}_1^t, \ldots, \mathbf{W}_{N_s}^t\right]^t$, and $\hat{\mathbf{x}}_a = \left[\hat{\mathbf{x}}_1^t, \ldots, \hat{\mathbf{x}}_{N_s}^t\right]^t$. The $\mathbf{W}_i$ weighting matrices are obtained by solving the following optimization problem:

$$\begin{array}{ll} \min\limits_{\mathbf{W}} & E\left[(\mathbf{W}^t\ \hat{\mathbf{x}}_a - \mathbf{x})(\mathbf{W}^t\ \hat{\mathbf{x}}_a - \mathbf{x})^t\right] \\ \text{s. to} & \sum\limits_{i=1}^{N_S} \mathbf{W}_i = \mathbf{I} \end{array} \tag{25}$$

where $E[\cdot]$ is the expectation operator, $\mathbf{x}$ is the vector of true values for the process state variables and $\mathbf{I}$ is the $n \times n$ identity matrix. Therefore, Problem (25) aims at minimizing the covariance of the estimation error $(\hat{\mathbf{x}}^* - \mathbf{x})$. In the case of specific interest in this PSSE application $N_s = 2$, so that Eq. (24) reduces to

$$\hat{\mathbf{x}}^* = \mathbf{W}_1^t\ \hat{\mathbf{x}}_1 + \mathbf{W}_2^t\ \hat{\mathbf{x}}_2 \tag{26}$$

It is possible to show that, for this particular case, the optimal estimate is given by [20],[21]:

$$\begin{array}{rl}\hat{\mathbf{x}}^* = & (\mathbf{P}_{22} - \mathbf{P}_{21})(\mathbf{P}_{11} + \mathbf{P}_{22} - \mathbf{P}_{12} - \mathbf{P}_{21})^{-1}\ \hat{\mathbf{x}}_1 + \\ & (\mathbf{P}_{11} - \mathbf{P}_{12})(\mathbf{P}_{11} + \mathbf{P}_{22} - \mathbf{P}_{12} - \mathbf{P}_{21})^{-1}\ \hat{\mathbf{x}}_2\end{array} \tag{27}$$

Equation (27) is known as *Bar-Shalom-Campo fusion formula* [22]. It can be further simplified if the individual estimates $\hat{\mathbf{x}}_1$ and $\hat{\mathbf{x}}_2$ can be assumed uncorrelated, yielding

$$\hat{\mathbf{x}}^* = \mathbf{P}_{22}\ (\mathbf{P}_{11} + \mathbf{P}_{22})^{-1}\ \hat{\mathbf{x}}_1 + \mathbf{P}_{11}\ (\mathbf{P}_{11} + \mathbf{P}_{22})^{-1}\ \hat{\mathbf{x}}_2 \tag{28}$$

B.Optimality Issues

It is possible to prove that, under certain conditions, the Decentralized Fusion Estimator provides the same results as a centralized (that is, a hybrid simultaneous) estimator that jointly processes the whole set of measurements made available by the N_S sets of sensors. This amounts to saying that no performance degradation is incurred by applying the decentralized strategy. As shown in [23], the above mentioned conditions are: *(i)* measurement errors must be uncorrelated across sensor sets, and *(ii)* the matrices that relate the measurement and state vectors in a linearized measurement model must have full column rank. In the PSSE problem involving both SCADA and PMU measurements, condition *(i)* is satisfied by assuming that SCADA and PMU metering channels are independent. Condition *(ii)* in principle implies that the electrical network must be both SCADA- and PMU-observable, although, as discussed in the sequel, the strict PMU-observability condition can be relaxed through the use of additional information at the PMU-based estimation stage.

C.Hybrid SCADA-PMU State Estimation as an Estimation Fusion Problem

If SCADA and phasor measuring systems are interpreted as distinct classes of sensors used for monitoring the same power network, the Multisensor Data Fusion concepts discussed in the previous subsection can be used to incorporate PMU measurements into PSSE. Accordingly, each of those monitoring systems processes its own measurement set in order to produce independent state estimates that reflect the current operating condition of the power system. The SCADA-based and PMU-based state estimators are hereafter referred to as SSE and PSE, respectively. In addition, let us denote by $\mathbf{z}_S$ and $\mathbf{z}_P$ the measurement vectors whose processing by SSE and PSE, respectively, produces states estimates $\hat{\mathbf{x}}_S$ and $\hat{\mathbf{x}}_P$, whose error covariance matrices are $\mathbf{P}_S$ and $\mathbf{P}_{P.}$ Matrices $\mathbf{P}_S$ and $\mathbf{P}_{P.}$ are computed by Eq. (5) using the appropriate Jacobian and measurement error covariance matrices.

Assuming that individual estimates $\hat{\mathbf{x}}_S$ and $\hat{\mathbf{x}}_P$ and corresponding error covariance matrices are available, they can be optimally combined in the Fusion Module of Figure 2. By adopting the reasonable assumption that the SCADA and PMU metering channels are independent, the optimal fused estimate can be obtained from Eq. (28) as

$$\hat{\mathbf{x}}^* = \mathbf{P}_P\ (\mathbf{P}_S + \mathbf{P}_P)^{-1}\ \hat{\mathbf{x}}_S + \mathbf{P}_S\ (\mathbf{P}_S + \mathbf{P}_P)^{-1}\ \hat{\mathbf{x}}_P \quad (29)$$

This estimator is referred to as *Fusion State Estimator* (FSE). It is interesting to notice from Eq. (29) that the matrix that actually defines the weight of each component estimate $\hat{\mathbf{x}}_S$ and $\hat{\mathbf{x}}_P$ in the optimal solution is the error covariance matrix associated with the other component. Since less accurate estimates lead to covariance matrix with larger values, better quality estimates receive larger weights, as one would expect.

The Bar-Shalom-Campo equation (29) is not amenable for application to large networks, due to the explicit matrix inversion on its right-hand side. There is, however, an alternative form for it that prevents those computational difficulties. By using Eq. (5) to define the SSE and PSE gain matrices $\mathbf{G}_S$ and $\mathbf{G}_P$, it is possible to show that Eq. (29) can be rewritten as:

$$\hat{\mathbf{x}}^* = (\mathbf{G}_S + \mathbf{G}_P)^{-1}\ \mathbf{G}_S\ \hat{\mathbf{x}}_S + (\mathbf{G}_S + \mathbf{G}_P)^{-1}\ \mathbf{G}_P\ \hat{\mathbf{x}}_P \quad (30)$$

so that

$$(\mathbf{G}_S + \mathbf{G}_P)\ \hat{\mathbf{x}}^* = \mathbf{G}_S\ \hat{\mathbf{x}}_S + \mathbf{G}_P\ \hat{\mathbf{x}}_P \quad (31)$$

Since gain matrices $\mathbf{G}_s$ and $\mathbf{G}_P$ are available from the individual SSE and PSE solutions, Eq. (31) can be solved by sparse triangular factorization and forward/back substitution.

D.Handling PMU-Observability Issues

Equation (29) requires the availability of both $\hat{\mathbf{x}}_S$ and $\hat{\mathbf{x}}_P$, which suggests that SCADA-observability and PMU-observability are both necessary conditions for applying the estimation fusion strategy. Observability with respect to SCADA measurements is usually granted in practice, but the same does not apply to PMU-observability, due to the still limited PMU penetration in power networks.

However, PMU-unobservability can be circumvented by incorporating complementary information into the PSE stage, in such a way as to artificially create the required observability conditions to compute $\hat{\mathbf{x}}_P$. Since that additional information is usually approximate and often inaccurate, it must be *critical* [13], [14], in order to avoid contaminating the estimates of the PMU-observable states. In addition, a judicious choice of the associated variance values should be exercised. In practice, those variances should take values that are some orders of magnitude larger than the telemeasurement variances. At the outcome of the PSE stage, those large entries will be reflected on the error covariance matrix $\mathbf{P}_P$, so that its diagonal values corresponding to the PMU-unobservable states will be also large. Since large variances lead to small weighting factors at the fusion step, the PSE estimates receive very small weights, so that the corresponding SSE estimates eventually prevail at fusion stage. As a consequence, the effects of the assumed complementary information are filtered out by the fusion process and have no significant effect on the optimal estimates.

There are basically two forms for adding the above mentioned complementary information: through pseudo-measurements or via *a priori* state information. In this paper we make use of *a priori* state information data, for two reasons: first of all, some kind of information on state variable values is always available, either as recently calculated state estimates or, lacking them, standard “expected” values for bus complex voltages. The second reason is computational: as discussed in Subsection III-A, G3M rotations can easily handle *a priori* information at initialization time, at virtually no computational cost.

V. Impact on Bad Data Analysis

Bad data analysis in the context of hybrid state estimation has been previously addressed in the literature [24]. However, the peculiar aspects of the non-conventional estimation architectures presented in this paper require a re-examination of the way bad data may affect the final state estimates.

Bad data methods in PSSE have been investigated through many years and are available in the literature [13], [14], [25]. They share as a common characteristic the requirement of a certain level of local measurement redundancy to ensure good performance. That knowledge can be taken advantage of by performing conventional bad data analysis at the first estimation module, using one of the reliable methods available. As a consequence, one would ensure that the SCADA-based estimates to be later combined with PMU-based information are free from the influence of bad data. However, performance still depends on the existence of adequate levels of local redundancy. Although that is usually granted for most regions comprising a given power network, there are often weak spots in which the available telemetered data is insufficient, so that critical measurements (whose gross errors are undetectable [14],[13]) and critical sets (whose gross errors are unidentifiable [25],[14],[13]) may occur.

In those cases, multistage estimation methods offer additional means to take advantage of the extra redundancy and enhanced accuracy provided by phasor measurements. In fact, depending on the location of the PMUs in the power network, estimation errors due to bad data on critical measurements and critical sets can be prevented through the use of multistage strategies, as illustrated in the next section of this paper.

VI. Simulation Results

To illustrate the application of the two multistage estimation strategies presented in this paper, several simulations have been carried out on the *IEEE* 30-bus and 57-bus benchmark systems. All simulations make use of a power flow study to generate the "true" values for the state and network variables. Measurements are generated by adding random Gaussian distributed errors to those values, with zero mean and variances corresponding to meter accuracies. Measurement errors are not allowed to exceed $\pm 2\sigma$ in order to avoid adding unintentional bad data to the measurement set. The assumed accuracy level for SCADA measurements is 1%, while 0.1% is used for PMU measurements, for both magnitude and angle. An orthogonal scalar state estimator is employed to process the SCADA measurements in the first stage, although there is no restriction concerning the estimation algorithm at that stage. For all cases, the metering schemes render the test systems observable with respect to SCADA measurements. The latter comprise active/reactive power injection, active/reactive power flow, and bus voltage magnitude measurements. The second stage processes phasor measurements from a number of PMUs placed throughout the system. It is assumed that each PMU measures the complex voltage at the bus where it is installed, along with the complex currents through all branches incident to it. In general, the PMU measurement sets themselves do not ensure network observability. It is assumed that the voltage phasor is always monitored at the reference bus, which is bus 1 for both networks. Reported results for each case are obtained by averaging the outcomes of one hundred performed simulations, each of which considering distinct measurement errors.

To evaluate the performance of the APSI-Blocked G3M and Fusion estimation strategies, their results are compared with corresponding ones obtained with two other estimators, namely, a conventional SCADA-based estimator and a hybrid simultaneous state estimator. Quantitative assessment of the results is based on: *(a)* the global state estimate mean errors for both bus voltage phase angle (in degrees) and magnitude (in pu), $\bar{\varepsilon}_\theta$ and $\bar{\varepsilon}_{|V|}$, respectively; and *(b)* the voltage metric (in pu) defined as [26]:

$$\bar{\varepsilon}_{\vec{V}} = \left(\sum_j \left| \vec{V}_j^{true} - \vec{V}_j^{est} \right|^2 \right)^{\frac{1}{2}} \tag{32}$$

where $\vec{V}$ and $\vec{V}_j^{est}$ are the "true" and estimated complex voltage at the j-th bus, respectively. The global state estimate mean errors $\bar{\varepsilon}_\theta$ and $\bar{\varepsilon}_{|V|}$ are computed by averaging over the number of state variables the mean errors computed for each state variable over the 100 simulations. Similarly, phasor $\vec{V}_j^{est}$ is the average of the estimates obtained from each sampled simulation.

A.Results for the IEEE 30-bus system

This section reports the results of case studies conducted with the IEEE 30-bus network. Table I summarizes the SCADA and PMU metering schemes. The notation used in the table is as follows: P(Q) stands for active (reactive) power injection measurements; t(u) refers to active (reactive) power flow measurements; and |V| stands for voltage magnitude measurements. All of the above are SCADA measurements. $\vec{V}$ ($\vec{I}$) represents voltage (current) phasor measurements. Phasor units are (arbitrarily) located at buses 1, 2, 25 and 27. Table I also shows the redundancy level ρ for both measurement systems, defined as the ratio between the number of scalar measurements and the number of state variables.

TABLE I. METERING SCHEME FOR IEEE 30-BUS TEST SYSTEM

	SCADA ($\rho_{SCADA} = 1.6$)					PMU ($\rho_{PMU} = 0.58$)	
Meas. type	P	Q	$\lvert V\rvert$	t	u	$\vec{V}$	$\vec{I}$
Amount	15	15	14	27	27	4	13

Global performance indices computed for each of the state estimators for this case study are given in Table II. The absolute values of individual state estimates' mean errors are plotted in Figs. 3(a) and 3(b) for bus voltage phase angles and magnitudes, respectively.

The global performance indices in Table II show the improvements of the two multistage strategies with respect to the conventional SCADA estimator results. The comparison between the APSI via blocked G3M and Fusion estimators

TABLE II. GLOBAL PERFORMANCE INDICES FOR THE 30-BUS SYSTEM

	SCADA	Blocked APSI	Fusion	Hybrid
$\bar{\varepsilon}_{\vec{V}}$	9.72×10^{-3}	7.72×10^{-3}	1.76×10^{-3}	1.73×10^{-3}
$\bar{\varepsilon}_{\lvert V \rvert}$	8.77×10^{-4}	5.81×10^{-4}	2.40×10^{-4}	2.36×10^{-4}
$\bar{\varepsilon}_{\theta}$	7.30×10^{-2}	4.85×10^{-2}	6.21×10^{-3}	6.15×10^{-3}

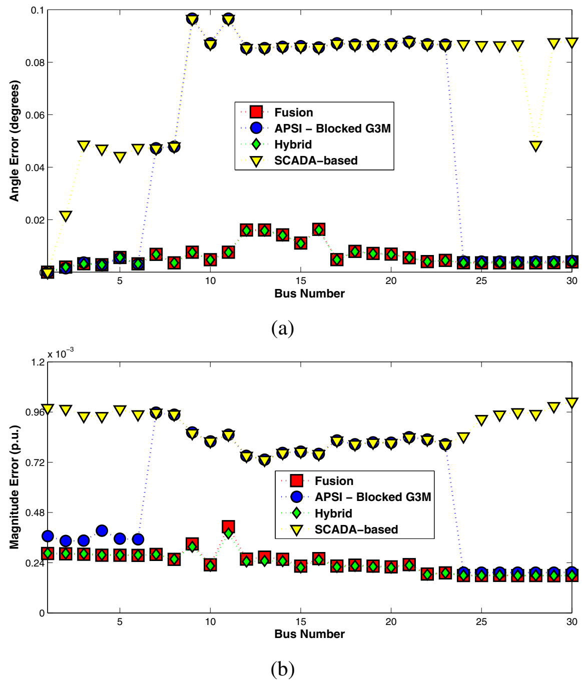

Fig. 3. Estimation errors for IEEE 30-bus system.

indicates that the latter tends to exhibit a better performance in terms of accuracy. In addition, it can be noticed that the Fusion results are very close to those provided by the Hybrid Centralized state estimator.

The individual estimates displayed in the plots of Fig. 3 allow a more detailed picture of the results. While the improvements provided by the blocked APSI scheme concentrate in the vicinity of the PMU locations and form clusters of more accurate estimates around those buses, the Fusion estimator is able to better spread the benefits of the phasor measurements throughout the network. This is due to fact that the Fusion strategy implemented according to Eq. (31) considers all correlations among the state variables. The plots also show that the Fusion estimates deviate very little from those obtained from a Hybrid Centralized estimator, despite the limited PMU penetration considered in this case, which does not ensure full PMU-observability for the 30-bus network.

B.Results for the IEEE 57-bus system

The SCADA and PMU metering schemes for cases B1 and B2 conducted on the 57-bus network are summarized in Table III. For case study B1, PMUs are arbitrarily located at buses 1, 2, 9, 10, 32, and 36, while case study B2 considers that PMUs are installed at all buses of the network, thus ensuring that it is fully PMU-observable. Table III also presents the corresponding SCADA and PMU redundancy indices.

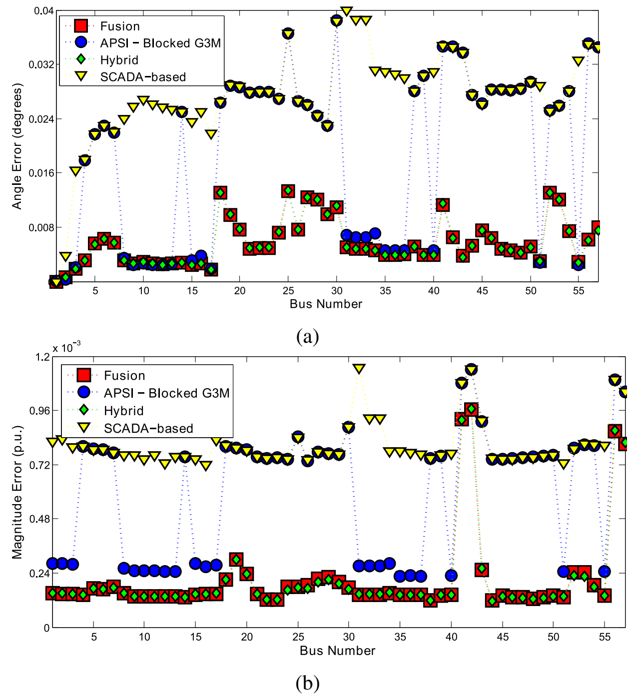

Fig. 4. Estimation errors for IEEE 57-bus system, Case B1.

1) Case B1 - PMU-unobservable network: The relatively low penetration of PMUs in this case does not render the system PMU-observable. In spite of that, the multistage estimation strategies are able to produce significant accuracy improvements with respect to the results of a conventional SCADA-based estimator, as shown by the performance indices in Table IV. The two plots in Figs. 4*a* and 4*b* represent the individual estimation errors for all bus voltage angles and magnitudes, respectively. The same pattern already observed for the 30-bus network applies to this case as well: the APSI-Blocked G3M estimates are significantly better than those yielded by the SCADA estimator at buses pertaining to the clusters defined by the PMU locations, and adhere to SCADA estimates elsewhere. On the other hand, estimates obtained with the Fusion strategy tend to closely follow those provided by the Hybrid Simultaneous estimator. In global terms, this tendency is confirmed by the corresponding performance indices in Table IV.

TABLE III. METERING SCHEMES B1 AND B2 FOR IEEE 57-BUS TEST SYSTEM

	SCADA $\rho_{SCADA} = 1.6$					PMU-B1 $\rho^{B1}_{PMU} = 0.5$		PMU-B2 $\rho^{B2}_{PMU} = 3.7$	
Meas. type	P	Q	$\lvert V \rvert$	t	u	$\vec{V}$	$\vec{I}$	$\vec{V}$	$\vec{I}$
Amount	24	26	28	53	53	6	21	57	156

TABLE IV. GLOBAL PERFORMANCE INDICES FOR THE 57-BUS SYSTEM - CASE B1

	SCADA	Blocked APSI	Fusion	Hybrid
$\bar{\varepsilon}_{\vec{V}}$	7.90×10^{-3}	6.46×10^{-3}	2.65×10^{-3}	2.64×10^{-3}
$\bar{\varepsilon}_{\lvert V \rvert}$	8.90×10^{-4}	5.99×10^{-4}	2.12×10^{-4}	2.11×10^{-4}
$\bar{\varepsilon}_{\theta}$	2.73×10^{-2}	1.86×10^{-2}	5.69×10^{-3}	5.69×10^{-3}

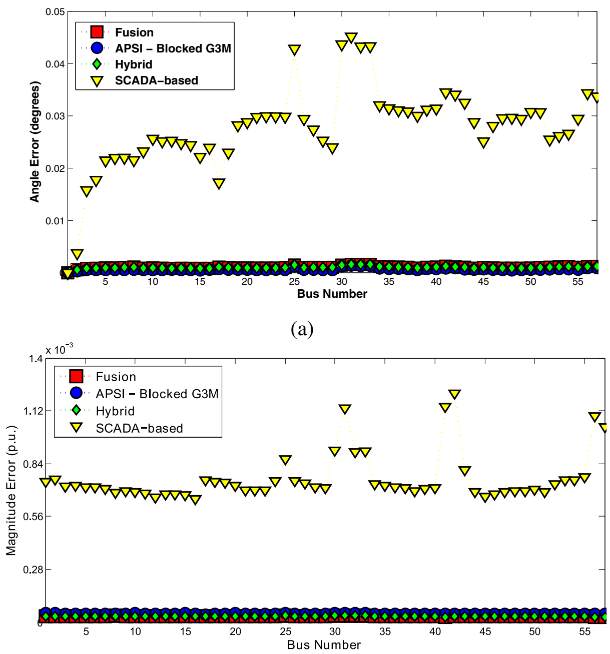

(a)

(b)

Fig. 5. Estimation errors for IEEE 57-bus system, Case B2.

2) Case B2 - PMU-observable network: This case corresponds to the ideal scenario in which the high penetration of PMUs by itself is sufficient to ensure network observability. Considering the superior quality of the phasor measurements, one then expects significant improvements in the accuracy level provided by all estimation strategies able to process that type of data. This is indeed confirmed by the global performance indices given in Table V, where the index values for both the multistage schemes and the hybrid simultaneous estimator are at least an order of magnitude less than those of the conventional SCADA-based estimator.

The above conclusion becomes still more apparent from the plots if Fig. 5, which individually compares estimate accuracies for both bus voltage angles (Fig. 5*a*) and magnitudes (Fig. 5*b*). Since the PMU metering scheme uniformly covers the entire network, the APSI-Blocked G3M estimator is now able to enhance the quality of the estimates for the states at every bus. For the same reason, it is possible to claim that the performance of the Estimation Fusion scheme in this case is optimal, in the sense that there is no performance degradation with respect to the hybrid centralized estimator, as already argued in Subsection IV-B. Indeed, that conclusion is apparent not only from the plots in Fig. 5, but also by comparing the global performance indices for both estimators in Table V, whose values practically coincide.

TABLE V. GLOBAL PERFORMANCE INDICES FOR THE 57-BUS SYSTEM - CASE B2

	SCADA	Blocked APSI	Fusion	Hybrid
$\bar{\varepsilon}_{\vec{V}}$	7.66×10^{-3}	3.65×10^{-4}	2.97×10^{-4}	2.97×10^{-4}
$\bar{\varepsilon}_{\vert V\vert}$	7.60×10^{-4}	4.42×10^{-5}	3.11×10^{-5}	3.10×10^{-5}
$\bar{\varepsilon}_{\theta}$	2.78×10^{-2}	6.48×10^{-4}	1.2×10^{-3}	1.20×10^{-3}

3) Case B3 - PMU-unobservable network, bad data in SCADA measurement set: This case is intended to illustrate how the extra redundancy provided by PMUs is able to mitigate the effects of bad data in the SCADA measurement set. The PMU metering scheme is the same as in Case B1, while the SCADA measurement set is slightly modified to create a low redundancy region near bus 16 of the 57-bus network. The metering schemes are summarized in Table VI. As a consequence of the changes, measurement $|V_{16}|$ becomes "SCADA-critical" in Case B3. In addition, that measurement is contaminated with a gross error of magnitude 10σ. The results for case B3 are presented in Table VII and Figs. 6 and 7.

TABLE VI. METERING SCHEME B3 FOR IEEE 57-BUS TEST SYSTEM

	SCADA $\rho_{SCADA} = 1.6$					PMU-B3 $\rho^{B3}_{PMU} = 0.5$	
Meas. type	P	Q	$\vert V\vert$	t	u	$\vec{V}$	$\vec{I}$
Amount	24	25	29	52	51	6	21

Since the measurement contaminated by the gross error is undetectable, the SCADA estimates are affected. This leads to a significant degradation of global indices $\bar{\varepsilon}_{\vec{V}}$ and $\bar{\varepsilon}_{|V|}$ for the SCADA estimator, as shown in Table VII. Figure 6 points out that the problem is due to the error in $|V_{16}|$, which clearly stands out against the other estimation errors (since the measurement is critical, there is little error propagation, with the exception of the attenuated cross-effect on θ_{16}). On the other hand, since phasor measurements are available near the affected bus, the influence of the gross error on the results of the multistage and hybrid estimators is only marginal, as also shown in in Table VII and Fig. 6.

TABLE VII. GLOBAL PERFORMANCE INDICES FOR THE 57-BUS SYSTEM - CASE B3

	SCADA	Blocked APSI	Fusion	Hybrid
$\bar{\varepsilon}_{\vec{V}}$	1.42×10^{-1}	6.95×10^{-3}	3.67×10^{-3}	3.22×10^{-3}
$\bar{\varepsilon}_{\vert V\vert}$	3.33×10^{-3}	6.40×10^{-4}	3.85×10^{-4}	3.14×10^{-4}
$\bar{\varepsilon}_{\theta}$	3.82×10^{-2}	2.80×10^{-2}	6.40×10^{-3}	6.20×10^{-3}

To better visualize the individual estimation errors of the APSI, Fusion and Hybrid simultaneous estimators, they are re-plotted in Fig. 7 without the SCADA results. A comparison of these plots with those in Fig. 4 clearly shows that the errors in both cases exhibit the same pattern, confirming that the multistage estimators are practically insensitive to the SCADA bad data under the above described conditions.

VII. Conclusions

This paper presents two novel multistage estimation approaches to incorporate phasor measurements into Power System State Estimation. A common feature of both methods is the treatment of SCADA and phasor data by distinct estimation modules, thus preventing the need of introducing significant changes to existing EMS software. Instead, the structure of conventional SCADA-based estimators are not affected, while the processing of phasor measurements and their integration

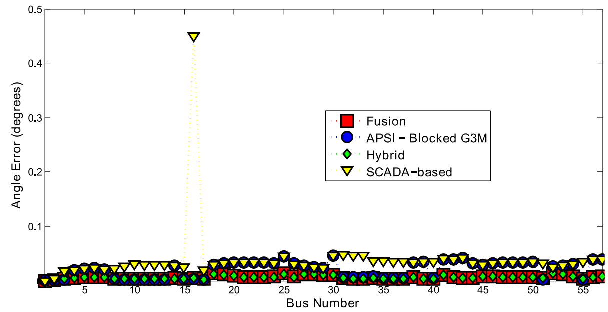

(a)

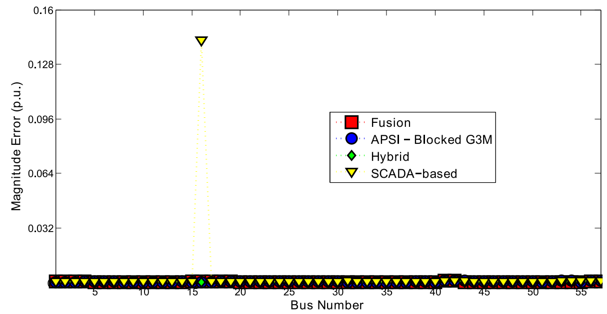

(b)

Fig. 6. Estimation errors for IEEE 57-bus system, Case B3.

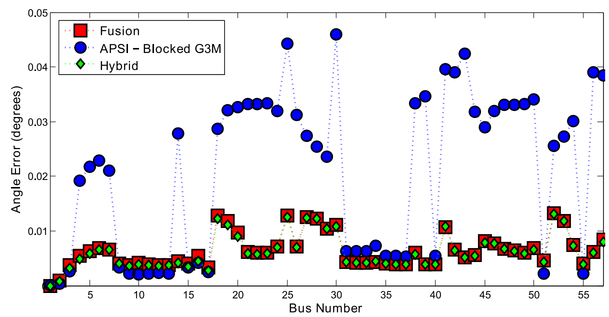

(a)

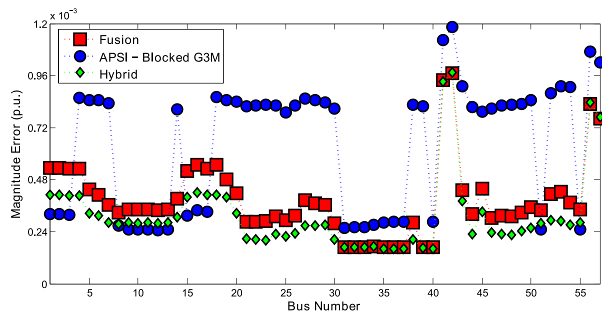

(b)

Fig. 7. Estimation errors for IEEE 57-bus system, Case B3, without SCADA estimator results.

with conventional estimates are performed by additional estimation modules. This decoupled strategy also recognizes the peculiar characteristics of both technologies, such as separate measuring channels and quite different sampling rates.

The proposed multistage estimators are based on different concepts. The first one considers conventional SCADA-based estimates as *a priori* information, which is processed along with phasor measurements by an orthogonal estimator. To take advantage of the linear relationships that result from formulating the estimation problem in rectangular coordinates, a blocked version of Givens rotations is employed. The second multistage estimator relies of principles borrowed from multisensor data function theory. Both strategies and their properties are described in detail, and several case studies conducted on two IEEE test systems are used to compare their performances with those of a conventional SCADA-based estimator and a hybrid simultaneous strategy. The results illustrate the distinguished features of each proposed approach, and the benefits of incorporating phasor measurements into power system real-time modeling.

ACKNOWLEDGEMENTS

The authors gratefully acknowledge the financial support of FINEP, a research & development funding agency of the Brazilian Ministry of Science and Technology, through the research grant for project “Novarede: The Electrical Network of the Future”. A. Simões Costa also acknowledges the support of CNPq, the Brazilian National Research Council.

References

[1] A. Bose. Smart transmission grid applications and their supporting infrastructure. *IEEE Transactions on Smart Grid*, 1(1):11–19, jun. 2010.

[2] Saikat Chakrabarti, Elias Kyriakides, Gerard Ledwich, and Arindam Ghosh. A comparative study of the methods of inclusion of pmu current phasor measurements in a hybrid state estimator. In *IEEE Power and Energy Society General Meeting*, pages 1 –7, Jul 2010.

[3] Simes Costa, A. and Leites, Renan da Costa. An Orthogonal State Estimator with Phasor Measurement Processing Capability. *III Brazilian Symposium of Electrical Systems, Belm, Par*, May 2010.

[4] A. G. Phadke, J. S. Thorp, R F Nuqui, and M. Zhou. Recent Developments in State Estimation with Phasor Measurements. *IEEE / PES Power Systems Conference and Exposition, 2009.*, Mar 2009.

[5] Yunzhi Cheng, Xiao Hu, and Bei Gou. A New State Estimation Using Synchronized Phasor Measurements. *International Symposium on Circuits and Systems*, pages 2817–2820, 18-21 May 2008.

[6] D.M. Bez and A. Simões Costa. Enhanced Probabilistic Modeling of Phasor measurement Errors in Hybrid SCADA-PMU State Estimation. In *Proceedings of the 12th PMAPS Conference*, pages 1–6, Istanbul, Turkey, June 2012.

[7] Ming Zhou, Virgilio A. Centeno, J. S. Thorp, and A. G. Phadke. An Alternative for Including Phasor Measurements in State Estimators. *IEEE Transactions on Power Systems*, 21(4):1930–1937, November 2006.

[8] Simes Costa, A. and Albuquerque, A. A two-stage orthogonal estimator to incorporate phasor measurements into power system real-time modeling. *17th Power Systems Computation Conference*, Stockholm, 2011.

[9] A. Simões Costa, A. Albuquerque, and D. Bez. An estimation fusion method for including phasor measurements into power system real-time modeling. *Power Systems, IEEE Transactions on*, PP(99):1, 2013.

[10] Antonio Simões Costa, Elizete Maria Lourenço, and Fabio Vieira. Topology Error Identification for Orthogonal Estimators Considering A

Priori State Information. *15th Power Systems Computation Conference*, 1:1–6, Liege, 2005.

[11] H.B. Mitchell. *Multi-Sensor Data Fusion: An Introduction*. Springer, 2007.

[12] F. C. Schweppe and J. Wildes. "Power System Static-State Estimation, Part I: Exact Model". *IEEE Trans. on Power Apparatus and Systems*, 3(4):120–135, Jan. 1970.

[13] A. Monticelli. *"State Estimation in Electric Power Systems: A Generalized Approach"*. Kluwer Academic Publishers, 1999.

[14] Ali Abur and Antonio Gmez Expsito. *Power system state estimation: theory and implementation*. Marcel Dekker, 2004.

[15] Peter Swerling. Modern state estimation methods from the viewpoint of the method of least squares. *IEEE Transactions on Automatic Control*, 16(6):707–719, December,1971.

[16] A. Simoes Costa and V.H. Quintana. An orthogonal row processing algorithm for power system sequential state estimation. *Power Apparatus and Systems, IEEE Transactions on*, PAS-100(8):3791 –3800, aug. 1981.

[17] W.M. Gentleman. Least squares computations by Givens transformations without square roots. *IMA Journal of Applied Mathematics*, 12(3):329, 1973.

[18] R. Zivanovic and C. Cairns. Implementation of pmu technology in state estimation: an overview. In *IEEE AFRICON 4th,*, volume 2, pages 1006 –1011, sep 1996.

[19] X.R. Li, Y. Zhu, J. Wang, and C. Han. Optimal linear estimation fusion. I. Unified fusion rules. *IEEE Transactions on Information Theory*, 49(9):2192–2208, 2003.

[20] Yunmin Zhu. *Multisensor Decision and Estimation Fusion*. Kluwer Academic, P.R. China, 1 edition, 2003.

[21] YM Zhu and X.R. Li. Best linear unbiased estimation fusion. In *Proceeding of 1999 International Conference on Information Fusion*, pages 1054–1061, Seattle, USA, July 1999.

[22] Yaakov Bar-Shalom and L. Campo. The Effect of the Common Process Noise on the Two-Sensor Fused-Track Covariance. *Aerospace and Electronic Systems, IEEE Transactions on*, AES-22(6):803 –805, nov. 1986.

[23] X. Rong Li and K. Zhang. Optimal Linear Estimation Fusion - Part IV: Optimality and Efficiency of Distributed Fusion. In *Proceedings of 4th International Conference on Information Fusion*, pages 1–8, Montréal, August 2001.

[24] G. N. Korres and N. M. Manousakis. State Estimation and Bad Data Processing for systems Including PMU and SCADA measurements. *Electric Power Systems Research*, 81:1514–1524, 2011.

[25] Th. Van Cutsem, M. Ribbens-Pavella, and L. Mili. Hypothesis testing identification: A new method for bada data analysis in power system state estimation. *IEEE Transactions on Power Apparatus and Systems*, PAS-100(11):3239 –3252, Nov. 1984.

[26] KEMA. Metrics for Determining the Impact of Phasor Measurements on Power System State Estimation. *Eastern Interconnection Phasor Project*, March 2006.